Dosimetric Estimates for Clinical Positron Emission Tomographic Scanning After Injection of [^{18}F]-6-Fluorodopamine

David S. Goldstein, Peter C. Chang, C. Bruce Smith, Peter Herscovitch, Sean M. Austin, Graeme Eisenhofer, and Irwin J. Kopin

Hypertension-Endocrine Branch, National Heart, Lung, and Blood Institute, Radiation Safety Branch, Division of Safety, Office of the Director, PET Section, Department of Nuclear Medicine, The Warren G. Magnuson Clinical Center, National Institutes of Health, Bethesda, Maryland, Clinical Neuroscience Branch, National Institute of Neurological Disorders and Stroke, Bethesda, Maryland; and Baker Medical Research Institute, Victoria, Australia

Positron emission tomographic (PET) scanning after systemic i.v. injection of fluorine-18-6-fluorodopamine ([^{18}F]-6F-DA) is a method for visualizing and measuring regional sympathetic nervous system innervation and function. Based on results of preclinical studies of rats and dogs and on previous literature about the fate of injected tracer-labeled catecholamines, dosimetric estimates for clinical studies are presented here. After injection of 1 mCi of [^{18}F]-F-DA, the radiation dose would be highest to the wall of the urinary bladder (1.40 rem/mCi), due to accumulation of radioactive metabolites of [^{18}F]-F-DA in urine. Radioactivity also would accumulate in bile. Organs receiving the next highest dose would be the kidneys (0.9 rem/mCi) and small intestine (0.2 rem/mCi). The parenchymal radiation dose would be lowest in the brain, since there is an effective blood-brain barrier for circulating catecholamines. Radiation doses to all organs after administration of 1 mCi of [^{18}F]-F-DA to humans would be less than 3 rem and, therefore, within current FDA guidelines.

J Nucl Med 1991; 32:102–110

The sympathetic nervous system is vital for maintaining homeostasis during stress (*1,2*). Alterations in sympathoneural activity may be pathologic in several neurocardiologic conditions (*3–11*), and many drugs act at sympathetic neuroeffector junctions.

Plasma levels of norepinephrine (NE), the sympathetic neurotransmitter, have been used to assess sympathoneural activity (*12–15*); however, the relationship between plasma NE levels and sympathetic activity is complex.

Radioiodinated metaiodobenzylguanidine (MIBG) has been used to visualize cardiac sympathetic innervation (*16–17*). Because the metabolic fate of MIBG differs from that of catecholamines (*18*), one cannot easily draw valid inferences about sympathetic function from MIBG scanning.

Positron emission tomographic (PET) scanning after systemic administration of fluorine-18-6-fluorodopamine ([^{18}F]-6F-DA) is a means for visualizing tissues with sympathetic innervation, especially in the heart. 6F-DA acts as a false neurotransmitter (*19–21*). After i.v. injection of [^{18}F]-6F-DA, striking images of the sympathetic innervation of the heart, spleen, and salivary glands are obtained, as the tracer is taken up and concentrated in vesicles in sympathetic nerve endings (*21* and Fig. 1). Analyses of myocardial radioactivity-time curves may also provide information about sympathetic function (*21*).

There has been no published description of the radiation doses that would be expected after administration of [^{18}F]-6F-DA into humans. This is the purpose of this communication.

The disposition of injected [^{18}F]-F-DA differs markedly from that of [^{18}F]-fluorodopa (*22,23*), and so estimates for radiation doses after administration of [^{18}F]-F-DA would be expected to differ from previously published estimates for [^{18}F]-6-fluorodopa (*24*).

MATERIALS AND METHODS

Studies of Rats

Thirty male Sprague-Dawley rats weighing 351 ± (s.e.m.) 2.8 g underwent insertion of heparinized polyethylene catheters (internal diameter 0.58 mm, external diameter 0.97 mm) into a carotid artery and femoral vein during pentobarbital anesthesia (50 mg/kg intraperitoneally).

Standards for 6F-DA, 6F-NE, 6F-dihydroxyphenylacetic acid, 6F-homovanillic acid, and 6F-normetanephrine were synthesized according to previously established methods (*25, 26*).

Tritium labeling of 6F-DA, with tritium on the carbon ring ([^{3}H]-6F-DA, 3.2 Ci/mmol) was conducted by New England

Received Nov. 3, 1989; revision accepted Jun. 11, 1990.
For reprints contact: Dr. David S. Goldstein, NHLBI, NIH, Building 10, Room 7N238, Bethesda, Maryland 20892.

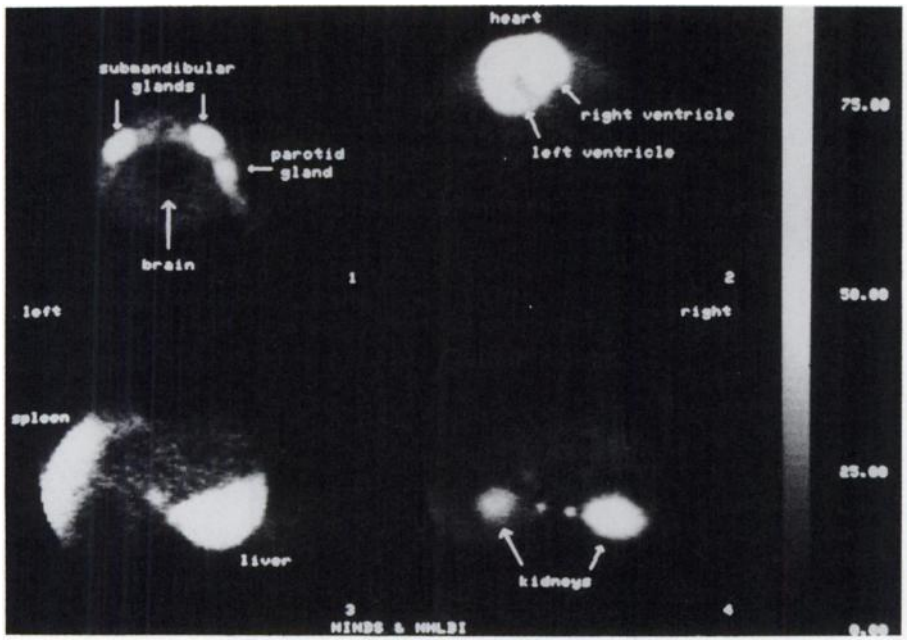

FIGURE 1
PET cross-sectional scans (10-min duration each) of the head, chest, upper abdomen, and lower abdomen ~1 hr after i.v. injection of 1.73 mCi of [^{18}F]-6-fluorodopamine into a pentobarbital-anesthetized dog. The heart, renal kidneys, liver, spleen, and salivary glands are visualized clearly, whereas there is little radiation in the brain, lungs, and chest wall.

Nuclear (Boston, MA, Lot No. 2557-062). The radionuclide was 60% radiochemically pure by liquid chromatography with liquid scintillation counting and was purified by alumina extraction (to 84% radiochemical purity) before use in the present study.

Ten microcuries of [^{3}H]-6F-DA was injected intravenously as a bolus. At 5, 10, 20, 60, and 120 min after the injection, arterial blood samples (3 ml) were obtained from groups of 6 animals each. The rats were then killed by pentobarbital overdose and tissues of the left ventricular apex, liver, spleen, kidney, and a salivary gland were excised. Arterial blood samples (1.5–3 ml) were obtained immediately before the animals were killed. The radioactivity in aliquots of 50 μl blood and 10 μl plasma was counted. The remaining plasma was separated into 200–500-μl aliquots and frozen at −70°C until assayed. Tissue samples (0.2–1.5 g) were frozen immediately in dry ice (−20°C), weighted, homogenized in 5–15 volumes of 0.4 N perchloric acid, and the supernatants stored at −70°C until assayed. Endogenous and fluorinated catechols in plasma (100–500 μl) and tissue supernatants (100–500 μl) were extracted by adsorption on alumina, eluted with acidified chromatographic mobile phase, and separated and quantified using reversed phase, ion-pairing liquid chromatography with electrochemical detection (*27,28*).

Studies of Dogs

An adult foxhound weighing ~25 kg and three beagles weighing ~12 kg underwent a total of seven PET scans. Each animal was anesthetized with pentobarbital, intubated, artificially respired, and underwent aseptic percutaneous insertion of femoral arterial and saphenous or forelimb venous catheters. Each dog, intubated but breathing spontaneously, was placed supine in the "Neuro-PET" head scanner or in the "PosiCam" body scanner (Positron Corp., Houston, TX). The arterial catheter was attached to a pressure transducer for continuous polygraphic recording of blood pressure and pulse rate. General anesthesia was maintained by occasional injections of pentobarbital. Each dog was monitored for ~2 hr, during which [^{18}F]-F-DA was synthesized. A baseline arterial blood sample (6 ml) was drawn and then the [^{18}F]-labeled compound injected intravenously over ~1 min. PET scans and blood samples were obtained up to 3 hr after the injection, and the durations of the scans and sampling were increased progressively from 5 min to up to 1 hr. In the foxhound and one beagle, the position of the dog in the scanner was changed frequently to visualize radioactivity at different levels. In the two other beagles, consecutive scans of the thorax and upper abdomen were obtained.

Fluorine-18-labeled F-DA was synthesized from [^{18}F]-labeled fluorodopa (fluorodihydroxyphenylalanine) by enzymatic decarboxylation of fluorodopa using a L-amino-acid-decarboxylase prepared from hog kidneys (*21*). The injectate contained ~1 mg of physiologically active dopamine and ~1 mCi of ^{18}F. The amount of radioactivity injected in each scanning session (range 0.7–2.0 mCi), depended on the yield of [^{18}F]-6F-DA. The radiochemical and mass purity of each aliquot was assayed and found to be at least 98% [^{18}F]-F-DA.

Data Reduction and Analysis

Results are presented as means ± s.e.m. A p value <0.05 defined statistical significance.

In the study of rats, computer-assisted statistical analyses (Statview 512+, Brainpower Inc., Calabasas, CA) included one-way analyses of variance (ANOVAs) to examine the significance of differences across time periods. In the event of non-homogeneity of variances, ANOVAs were conducted on log-transformed data.

In the PET study of dogs, the PET images were reconstructed with correction for attenuation and for the physical decay of the tracer (the physical half-life of ^{18}F is 1.83 hr), stored on magnetic tape, restored for analysis using a Digital Equipment Corporation VAX computer (Malvern, MA) and analyzed using the Medical Imaging Retrieval, Analysis and Graphics (MIRAGE) software system, developed by the nuclear medicine department.

Time-activity curves related the log of the tissue radioactiv-

ity concentration to time after injection of the tracer. To compare results among animals, tissue radioactivity concentrations were adjusted for the amount injected and the weight of the animal, and so the unit of tissue radioactivity was nCi-kg/cc-mCi. For plasma or blood, time-activity curves were derived from direct assays of the radioactivity concentrations in aliquots of centrifuged or uncentrifuged arterial blood. Time-activity curves for organ radioactivity were based on circular regions of interest occupying about half the width of the imaged organ.

Bi-exponential equations of best fit were calculated using the interactive "BLD" curve analysis program of the nuclear medicine department. Graphic analyses were performed on a Macintosh II computer using CricketGraph (Cricket Software, Malvern, PA) and on a VAX computer (Digital Equipment Corp.).

Dosimetric estimates were based on the present studies of rats and dogs and previously published data about the fate of systemically injected tritium-3- or carbon-14- (^{14}C)-labeled dopamine, other radiolabeled non-fluorinated catecholamines (e.g., *29–32*), unlabeled 2- or 6F-DA, or [^{3}H]-2-F-DA (*20*). The dose calculations were made using the MIRDOSE (Oak Ridge Associated Universities version of January, 1988) computer program.

RESULTS

Studies of Rats

Five minutes after administration of [^{3}H]-6F-DA, the amount of circulating [^{3}H]-6F-DA was decreased to less than 3% of total plasma ^{3}H, and ^{3}H concentrations in the ventricular myocardium, spleen, salivary gland, kidney, and liver averaged 8, 3, 2, 14, and 4 times that of blood (Fig. 2).

Tissue:blood ratios of ^{3}H increased progressively over time. By 120 min after injection of the tracer, tissue:blood ratios of ^{3}H in myocardium, spleen, salivary gland, kidney, and liver were increased by factors of 60, 20, 12, 19, and 7. Between 5 and 120 min after the injection of [^{3}H]-6F-DA, tissue:plasma ratios of ^{3}H also increased in the heart, spleen, and salivary glands (Fig. 2).

In organs with dense sympathetic innervation (heart, spleen, and salivary glands), decreases in tissue ^{3}H were relatively slow between 5 and 120 min after the injection and followed a monoexponential pattern of decline (Fig. 2). The half-time values were 183 min in the heart, 168 min in the spleen, and 109 min in the salivary gland. In contrast, in organs involved with excretion (liver, kidney, blood, and plasma), the decreases in tissue ^{3}H were relatively fast, and the half-time values based on a monoexponential decline were small (Table 1). The rates of decline of ^{3}H concentrations were similar in the kidney and blood between 60 and 120 min after injection of [^{3}H]-6F-DA.

In the heart, the majority of the tissue ^{3}H contents were in ^{3}H-catechols—especially [^{3}H]-6F-DA and [^{3}H]-6F-NE; in the kidney and liver, the contributions of [^{3}H]-6F-DA and [^{3}H]-6F-NE to the total concentrations

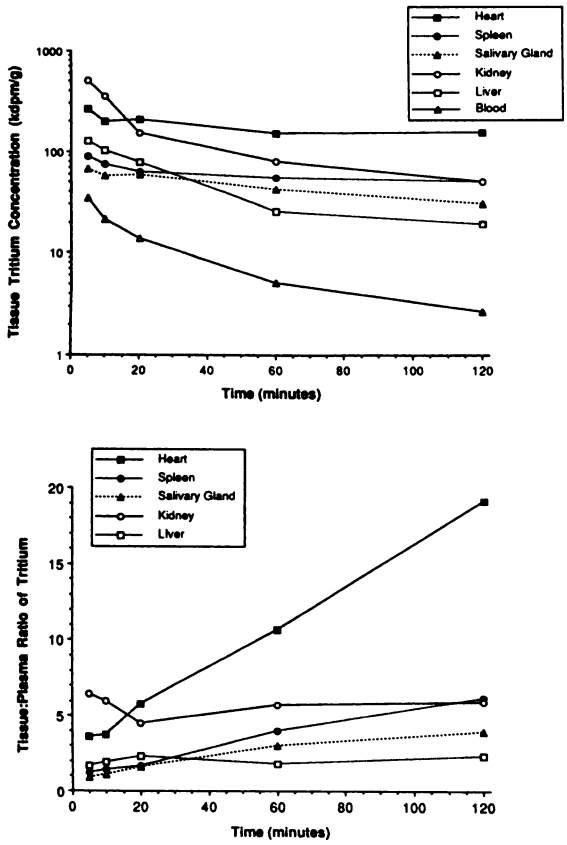

FIGURE 2
Tissue tritium concentrations (upper panel) and tissue:plasma ratios of tritium (lower panel) after injection of [^{3}H]-6F-DA into rats. Each point represents data from six different animals.

of ^{3}H remained below 30%. In marked contrast, plasma concentrations of [^{3}H]-6F-NE were barely detectable at all time points after injection of [^{3}H]-6F-DA.

Concentrations of endogenous catechols in plasma were unchanged after the injection of [^{3}H]-6F-DA, except that after 120 min, plasma NE, epinephrine, and dopa levels increased as the pentobarbital anesthesia wore off.

Studies of Dogs

Concentrations of ^{18}F in blood and plasma decreased rapidly after injection of [^{18}F]-F-DA (Fig. 3). The mean biologic half-time of blood [^{18}F] between 1 and 4 min after injection was 1.5 min. Thereafter, the rate of disappearance of total plasma ^{18}F became much slower; between 10 and 60 min after the injection, the mean half-time averaged 32 min.

Plasma total concentrations of 6F-DA fell rapidly after injection of [^{18}F]-F-DA, with a half-time of ~1.5 min, i.e., at the same rate as ^{18}F. Therefore, within a few minutes of the injection, most of the ^{18}F in plasma was not itself due to the tracer.

In five studies, the plasma:blood radioactivity ratio invariably increased progressively during the scanning

TABLE 1
Kinetic Parameters for Tissue Concentrations of ^{3}H After Intravenous Injection of [^{3}H]-6-Fluorodopamine into Anesthetized Rats (n = 6)

Organ	Slope	k (1/min)	t-½ (min)	y-Intercept (kdpm/g)	y-Intercept (nCi-cc/ kg/mCi)
Heart	0.0016	0.004	184	290	3955
Spleen	0.0018	0.004	168	100	1364
Salivary gland	0.0028	0.006	109	70	955
Kidney	0.0080	0.018	38	730	9955
Liver	0.0072	0.017	42	140	1909
Blood	0.0090	0.021	33	—	—
Plasma	0.0080	0.019	37	—	—

Slope = slope of line of best fit relating the log of the tissue concentration of ^{3}H (kdpm/g) to time (min); t-½ = mono-exponential half-life.

session, from a minimum value of less than 0.8 to a maximum value of about 1.4.

After injection of [^{18}F]-6F-DA, there was intense positron emission from the renal pelvis, heart, liver, kidneys, spleen, and salivary glands, with little positron emission from the brain, lungs, and skeletal muscle (Fig. 1).

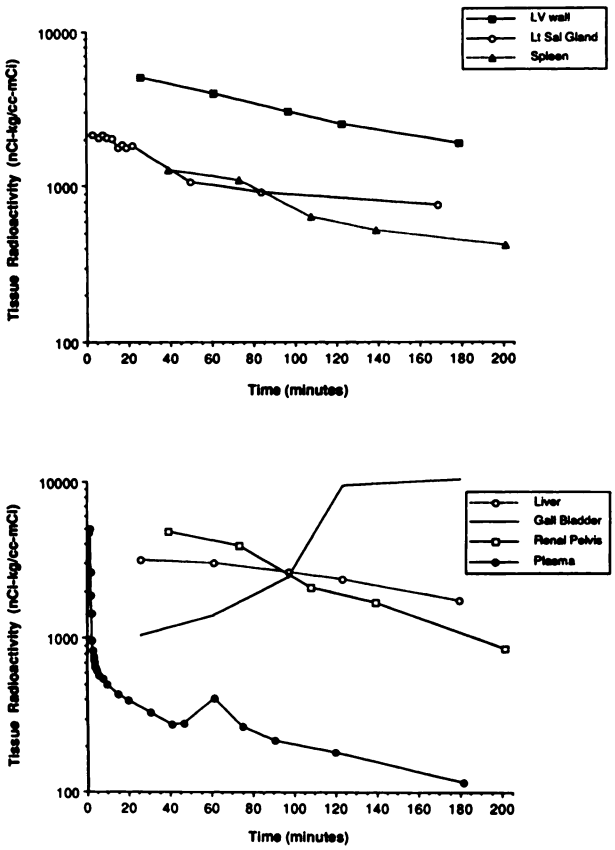

FIGURE 3
Tissue radioactivity concentrations after injection of [^{18}F]-6-fluorodopamine into an anesthetized dog. Upper panel shows data for organs with known dense sympathetic innervation (heart, salivary glands, spleen) and lower panel data for organs involved with excretion (plasma, liver, gall bladder, renal pelvis).

After initial distribution, the tissue radioactivity generally declined biexponentially in the heart, liver, spleen, salivary glands, renal pelvis, and plasma (Figs. 3 and 4), whereas radioactivity accumulated progressively in the gall bladder in all the PET studies (Fig. 3). Virtually immediate appearance of radioactivity in the renal pelvis demonstrated that a portion of the injected tracer was rapidly filtered and excreted. Thereafter, renal pelvic radioactivity decreased rapidly, with a biologic half-time similar to that of ^{18}F in plasma in 2 of 3 dogs.

During the 3 hr after injection of [^{18}F]-6F-DA, myocardial radioactivity decreased with mean biologic half-time values of 22 ± 4 and 135 ± 24 min (n = 7). The rate of disappearance of radioactivity from the left ventricular wall was slower than that from plasma, so that the ratio of ventricular-to-plasma radioactivity increased progressively to an average maximum value of 9. The myocardial load of radioactivity, obtained by adding the y-intercept values for the rapid and slow components, averaged 5521 nCi-kg/cc-mCi.

The basis for estimates of radioactivity load and effective half-times for several organs are explained in the Discussion. The estimated radiation doses calculated using the MIRDOSE program are summarized in Table 3.

DISCUSSION

Plasma Radioactivity After Injection of [^{18}F]-6F-DA or [^{3}H]-6F-DA

After injection of [^{3}H]-6F-DA into rats and [^{18}F-]6F-DA into dogs, plasma levels of the tracers declined rapidly (half-time < 1.5 min during the early phase), consistent with previous findings (*33,34*). Catecholamines are removed from plasma mainly by extraneuronal uptake (uptake-2, (*35*), Fig. 5), with subsequent intracellular metabolism to oxygen-methylated derivatives (*29–32*). A proportion of circulating dopamine is taken up by sympathetic nerve terminals (uptake-1). Axoplasmic dopamine can be translocated into storage vesicles and converted to NE (*20*). Vesicular storage of [^{18}F]-6F-DA and [^{18}F]-6F-NE is thought to be the basis for visualization of organs with sympathetic innervation by PET (*21*).

By 60 min after injection of [^{14}C]dopamine, [^{3}H] dopamine, or [^{3}H]-6F-DA into rats, most of the radioactivity in plasma is due to oxygen-methylated metabolites of NE (*33* and unpublished observations). After injection of [^{18}F]-6F-DA, the initial decline in plasma radioactivity probably represents rapid entry of the tracer into the extracellular fluid space and then into sympathetic nerve endings and nonneuronal cells. The slower, later decline in plasma radioactivity probably

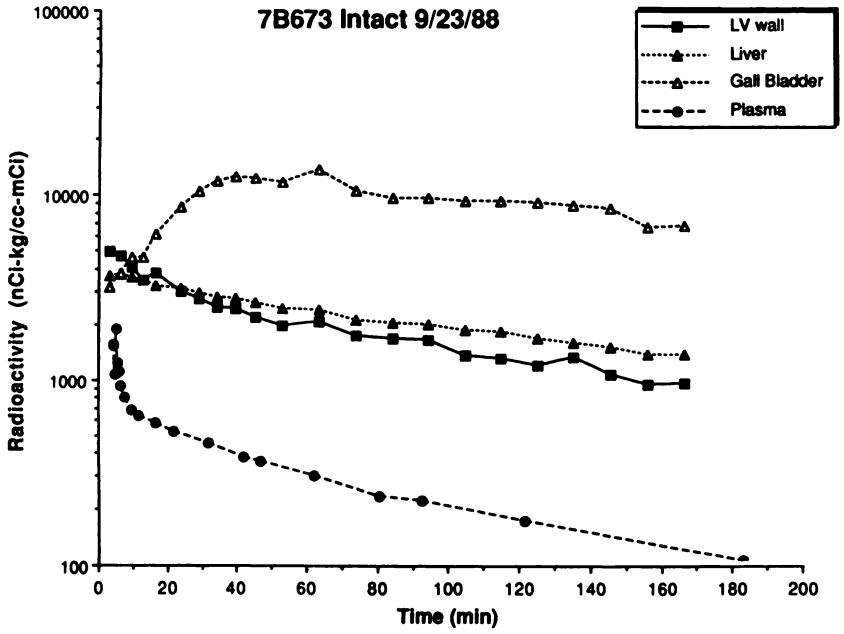

FIGURE 4
Tissue radioactivity concentrations after injection of [^{18}F]-6-fluorodopamine into an anesthetized dog.

represents clearance due to excretion of metabolites of [^{18}F]-F-DA and of [^{18}F]-NE (*21*).

Radiation Dosimetric Estimates for Specific Organs

After injection of [^{18}F]-6F-DA, the initial radioactivity load depends on organ blood flow and mass and on the avidity of uptake-1 and uptake-2. In tissues where the amine is stored as [^{18}F]-6F-DA or [^{18}F]-6-NE, the rate of release of these compounds would eventually determine the biologic half-time, whereas in tissues responsible for excretion, such as the liver and urinary tract, the radiation dose would depend on the rate of excretion of the metabolites. For each organ, dosimetric calculations require estimates of the effective half-time of ^{18}F (Table 2).

Bladder

Accumulation of radioactivity in the bladder would be an important aspect of radiation dosimetry (Tables 3 and 4). Based on results using other tracer-labeled catecholamines (*16,30–32*), by 2 hr after the end of an infusion of [^{18}F]-6F-DA, over 60% of the administered radioactivity would be in bladder urine. Virtually all the urinary radioactivity would be in the form of physiologically inactive oxygen-methylated metabolites of dopamine or of NE (*33*). In clinical protocols, the

FIGURE 5
Diagrammatic representation of the fate of injected [^{18}F]-fluorodopamine (^{18}F-DA) in a sympathetic nerve ending and a nonneuronal cell. Fluorine-18-DA actively removed into the axoplasm by Uptake-1 can be metabolized by mitochondrial monoamine oxidase to form [^{18}F]-dihydroxyphenylacetic acid (^{18}F-DOPAC) or taken up into vesicles containing dopamine-β-hydroxylase (DBH) and converted to [^{18}F]-norepinephrine (^{18}F-NE). Fluorine-18-DA removed into nonneuronal cells by Uptake-2 can be converted to O-[^{18}F]-methoxytyramine (O-Me ^{18}F-DA). Fluorine-18-DOPAC formed extraneuronally or taken up after release from sympathetic neurons is converted to [^{18}F]-homovanillic acid (^{18}F-HVA) by catechol-O-methyltransferase (COMT). Uptake of [^{18}F]-fluorodopamine into sympathetic nerve endings, with conversion to and storage of [^{18}F]-fluoronorepinephrine in vesicles, results in concentration of radioactivity in sympathetically innervated tissues.

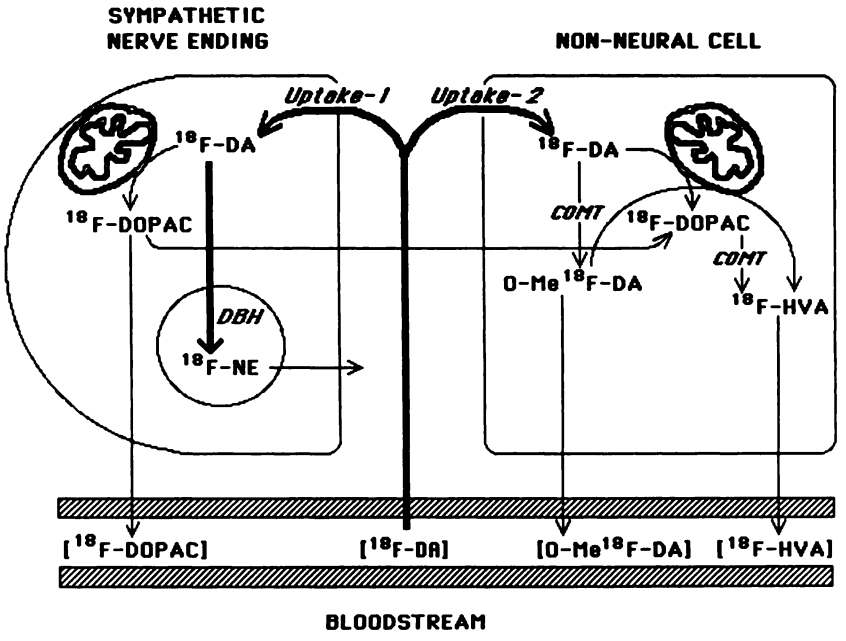

TABLE 2
Estimated Organ Radioactivity Loads and Effective Half-Lives After Injection of [^{18}F]-6-Fluorodopamine into Anesthetized Dogs

Organ	Estimated radioactive load (% dose)	Estimated effective half-life (hr)
Heart	4.0	0.8
Liver	12.5	1.0
Lungs	0.0	N/A
Spleen	0.4	0.9
Gut wall	18	1.0
Adrenals	0.2	1.8
Brain	0.0	N/A
Kidneys	29	0.6
Skeletal muscle and skin	22	1.0
Uterus	0.3	1.0
Testes	0.0	N/A
Renal filtration of dopamine	2.0	1.8
Plasma	1.0	0.7
Other	11	0.7
Total	100	—

subject would probably urinate about 3.5 hr after injection of [^{18}F]-6F-DA. About 60% of the injected radioactivity would appear in urine by 3.5 hr after injection (*29,30*), with the effective half-time equal the physical half-time of ^{18}F.

Kidneys

The kidneys received ~25% of the cardiac output (*36*), and the fractional renal extraction of circulating catecholamines is ~65% (*37,38*). If [^{18}F]-6F-DA were administered as an immediate bolus, and if the lungs removed none (see below), then ~55% of the administered [^{18}F]-6F-DA would be removed in the body as a whole (*37*), so that after several recirculations, the kidney would remove about 29% of the administered dose. The residence time of [^{18}F]-6F-DA in the kidney is so short, the biologic half-time of the radioactivity would largely determine the radioactivity in pelvic urine. Due to the continuous excretion of radioactive metabolites, the pelvic urine radioactivity concentration would decline slowly in a manner roughly parallel to the decline in plasma radioactivity. If the kidney served as a conduit between the plasma and bladder urine, then the ratio of renal pelvic to plasma radioactivity would approach a constant value within ~60 min (see Appendix).

Based on analysis of the renal pelvic time-activity curves in two dogs in the present study, ~3% of the tracer was excreted almost instantaneously, consistent with the findings of Hempel et al. (*39*).

Gut

After injection of [^{18}F]-6F-DA into dogs, only low concentrations of radioactivity were found in regions

TABLE 3
Estimated Radiation Dose by Organ (Using the Results from Table 2)

Target organ	Total dose (rad/mCi)	% Primary contributor	% Secondary contributor
Urinary bladder wall	1.40	Urinary bladder contents (99)	Small intestine (0)
Kidneys	0.60	Kidneys (97)	Small intestine (1)
Small intestine	0.23	Small intestine (85)	Urinary bladder contents (7)
Adrenals	0.21	Adrenals (84)	Kidneys (1)
Gallbladder wall	0.17	Bile (75)	Small intestine (6)
Uterus	0.16	Urinary bladder contents (61)	Uterus (2)
Liver	0.08	Liver (78)	Kidneys (9)
Ovaries	0.07	Urinary bladder contents (53)	Small intestine (2)
LLI	0.07	Urinary bladder contents (62)	Small intestine (2)
ULI	0.07	Small intestine (52)	Urinary bladder contents (1)
Heart wall	0.06	Heart wall (81)	Muscle (5)
Spleen	0.05	Spleen (42)	Kidneys (3)
Testes	0.04	Urinary bladder contents (75)	Total body (1)
Pancreas	0.04	Kidneys (35)	Total body (1)
Total body	0.03	Urinary bladder contents (33)	Muscle (1)
Marrow	0.03	Total body (26)	Urinary bladder contents (2)
Stomach	0.03	Total body (24)	Kidneys (2)
Muscle	0.03	Urinary bladder contents (43)	Muscle (2)
Bone surface	0.02	Total body (34)	Urinary bladder contents (2)
Lungs	0.02	Total body (39)	Muscle (2)
Skin	0.01	Total body (35)	Urinary bladder contents (2)
Thymus	0.01	Total body (44)	Muscle (2)
Breasts	0.01	Total body (56)	Muscle (1)
Thyroid	0.01	Total body (56)	Muscle (3)
Brain	0.01	Total body (90)	Muscle (9)

ULI = upper large intestine; LLI = lowr large intestine. Numbers in parentheses indicate percentage.

TABLE 4
Information for Dynamic Bladder Model

Compartment	%Dose	$t_{½biol}$ (hr)
Heart	4.0	1.42
Liver	12.5	2.20
Spleen	0.4	1.77
Gut (small intestine)	18.0	2.20
Kidneys	29.0	0.89
Muscle	22.0	2.20
Uterus	0.3	2.20
Other	10.7	0.89

corresponding to small intestine, undoubtedly because of the large volume.

Adrenals

Normal adrenomedullary tissue takes up only a small proportion of catecholamines from the bloodstream because of the small percent of the cardiac output distributed to the adrenals and possibly because of relatively little uptake-1 activity (*40,41*). PET scanning after injection of [^{18}F]-6F-DA into dogs failed to detect adrenal radioactivity. If the adrenal radioactivity loading concentration were the same as for the liver (*42*), then for an adrenal weight of 8 g (*43*), the load would be ~0.2% of the injected amount. Since [^{18}F]-6F-DA could be converted to [^{18}F]-6-fluoroNE and stored as such for prolonged periods, a conservative estimate for the effective half-time of adrenal radioactivity would be the physical half-time of ^{18}F.

Gallbladder

The gallbladder may be viewed as a thin-walled sac containing the products of hepatic excretion. After injection of a mean of 1.8 mCi of [^{18}F]-6F-DA into intact dogs, gallbladder radioactivity invariably increased, probably due to a faster rate of release of radioactive [^{18}F]-6F-DA metabolites by the liver into the gallbladder than release of the bile into the small intestine; resorption of bile fluid would augment the increases in radioactivity concentration.

Bile flow averages about 500 ml/day in a 70-kg human (*44*). Since in dogs 1% of the total radioactivity in systemically injected radiolabeled dopamine is recovered in feces (*29*), whereas about 9% of the administered [^{18}F]-6F-DA is taken up by the liver, biliary excretion would represent only a small proportion of the excretion of the hepatic metabolites, with the majority being excreted via the kidneys. Since the gallbladder might not empty during the testing session, a conservative estimate of the effective half-time of ^{18}F in bile would be the physical half-time.

Reproductive Organs

Although it is possible that circulating catecholamines are removed by reproductive organs (testes, uterus, and ovaries), most of the radiation dose to these organs would be from radioactivity in bladder urine.

Liver

Hepatic delivery of [^{18}F]-6F-DA was estimated (*45*) to be ~12.5% of the injected dose and the effective half-time ~1.0 hr. After injection of [^{3}H]-6F-DA into rats, the initial hepatic load of radioactivity was ~1900 nCi-cc/kg-mCi and the effective half-time ~40 min. Both values therefore were somewhat less than in the dogs. After systemic injection of radiolabeled epinephrine into cats, hepatic radioactivity accounts for up to 22% of the infused dose (*32*).

Heart

The initial radioactivity load to the heart averaged about 5000 nCi-kg/cc-mCi, or ~4% of the injected radioactivity (*45*). Similarly, Kirshner (*32*) reported that at 2 min after i.v. injection of radiolabeled epinephrine into cats, a mean of 4.1% of the injected radioactivity was in cardiac tissue. In the present study of rats receiving [^{3}H]-6F-DA, the initial radioactivity load to the heart averaged 3955 nCi-cc/kg-mCi, a value ~20% less than that in dogs receiving [^{18}F]-6F-DA.

After [^{18}F]-6F-DA injection in dogs, the mean biologic half-time of cardiac radioactivity was ~1.5 hr, and so the effective half-time in the heart was ~0.8 hr. In rats receiving [^{3}H]-6F-DA, the biologic half-time was longer—~3 hr. Values for the S-factor used in the dosimetric estimates for the heart were obtained from the tables of Coffey and Watson (*47*).

Spleen

In rats receiving [^{3}H]-6F-DA, the splenic load of radioactivity averaged 1364 nCi-cc/kg-mCi, less than that in dogs receiving [^{18}F]-6F-DA (2082 nCi-cc/kg-mCi in 2 dogs). Kirshner (*32*) reported that at 2 min after systemic injection of radiolabeled epinephrine into cats, spleen radioactivity accounted for a mean of about 1.3% of the total dose.

Skeletal Muscle and Skin

Blood flow to skeletal muscle, skin, connective tissue, and fat averages about 25% of the cardiac output (*36, 46*). Assuming that 50% of the delivered catecholamines are removed in the limbs (*38*), about 12.5% of the administered dose would be removed in the first pass, with a total removal of about 22%.

Lungs

During infusions of [^{3}H]NE to a steady-state in humans, we have not observed any difference in pulmonary artery and peripheral arterial levels of [^{3}H]NE (unpublished observations), indicating little if any extraction of circulating catecholamines in the lungs. In dogs receiving [^{18}F]-6F-DA intravenously, radioactivity was not detected by PET scans in regions corresponding to the lungs. Therefore, the radioactive dose to the lungs due to uptake of the tracer would be very small.

Total Body

In the present study of dogs, uptake of [^{18}F]-6F-DA by the above organs did not account for about 11% of

the injected radioactivity. The y-intercept value for the relationship between the log of the plasma radioactivity concentration and time, beginning 20 min after injection in order to include mainly the elimination phase, was 52 nCi-kg/cc-mCi, or 86 nCi/cc. The plasma load of radioactivity would be only about 1% of the injected radioactivity. The remaining 10% therefore would be due to uptake by organs other than those listed or due to any binding of radioactivity to blood components. In dogs, the estimated effective half-time of plasma radioactivity after i.v. injection of [^{18}F]-6F-DA was 0.7 hr; in rats, the elimination half-time of plasma radioactivity after intravenous injection of [^{3}H]-6F-DA was ~0.5 hr.

Brain

Little if any radiation is expected to accumulate in the central nervous system after systemic injection of [^{18}F]-6F-DA (*21,22,32*).

CONCLUSIONS

The present results lead to the prediction that after injection of 1 mCi of [^{18}F]-6F-DA into humans, the radiation dose would be highest to the wall of the urinary bladder (1.40 rem/mCi), due to accumulation of radioactive metabolites of [^{18}F]-F-DA in urine, and lowest to the brain, since there is an effective blood-brain barrier for circulating catecholamines. Organs receiving the next highest doses would be the kidneys (0.9 rem/mCi) and small intestine (0.2 rem/mCi). Radiation doses to all organs would be less than 3 rem and therefore within current FDA guidelines.

Among the various organs studied, the relative loads of radiation and relative values for effective half-time were similar in rats and dogs; however, the results for rats differed from those in dogs, in that absolute radiation loads to all organs except the kidney were smaller in rats, and the rates of decline of renal and circulating radioactivity were faster in rats. These differences would be expected from the higher cardiac index of rats than dogs or humans. The species differences observed in the present study suggest that dosimetric estimates for PET studies involving administration of [^{18}F]-6F-DA in humans may require modification when actual clinical results are obtained.

APPENDIX

The Ratio of Renal Pelvic-to-Plasma Radioactivity Approaches a Constant Value After Injection of [^{18}F]fluorodopamine

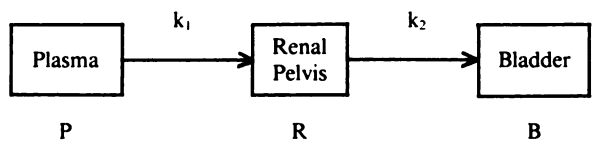

If the plasma radioactivity concentration declines bi-exponentially, then

$$P = A\,e^{-m_1 t} + B\,e^{-m_2 t}.$$

From the above model, $dR/dt = k_1P - k_2R$, $dR/dt + k_2R = k_1P$.
Multiplying both sides by $e^{k_2 t}$:

$$e^{k_2 t}\,dR/dt + k_2 e^{k_2 t}\,R = Pk_1\,e^{k_2 t}P.$$

Since $d(AB)/dt = A\,(dB/dt) + B\,(dA/dt)$,

$$d(R\,e^{k_2 t})/dt = k_1\,e^{k_2 t}P = k_1 e^{k_2 t}\,(A\,e^{-m_1 t} + B\,e^{-m_2 t})$$
$$= k_1\,A\,e^{(k_2-m_1)t} + k_1\,B\,e^{(k_2-m_2)t}$$

Integrating, $Re^{k_2 t} = [(k_1A/\{k_2-m_1\})]e^{(k_2-m_1)t} + [(k_1B/\{k_2-m_2\})]e^{(k_2-m_2)t} + c$,

where $c = -[(k_1A/\{k_2-m_1\}) + (k_1B/\{k_2-m_2\})]$ and
$R = (k_1/\{k_2-m_1\})\,A\,e^{-m_1 t} + (k_1/\{k_2-m_2\})\,B\,e^{-m_2 t} + ce^{-k_2 t}$.
Since $P = A\,e^{-m_1 t} + B\,e^{-m_2 t}$, then if $k_2 > m_1 >> m_2$, R/P approaches k_1/k_2.
Alternatively, $dR/dt = k_1P - k_2R$, $P = (1/k_1)\,(dP/dt)$ $dB/dt = k_2R$, $R = (1/k_2)\,(dB/dt)$.
If V_B is the volume of the bladder and V_P the apparent volume of distribution of the radioactivity in the plasma, and if radioactivity enters B as rapidly as it leaves P, $V_B\,(dB/dt) = V_P\,(dP/dt)$.
Therefore,

$$R/P = (k_1/k_2)\,(V_P/V_B).$$

REFERENCES

1. Cannon WB. *Bodily changes in pain, hunger, fear and rage.* New York: Appleton; 1929.
2. Goldstein DS. Stress-induced activation of the sympathetic nervous system. In: Grossman A, ed. *Neuroendocrinology of stress.* East Sussex, England: Bailliere Tindall; 1987:253–278.
3. Esler M, Jennings G, Lambert G. Noradrenaline release and the pathophysiology of primary human hypertension. *Am J Hypertens* 1989;2 (suppl 3 Pt. 2): 140S–146S.
4. Goldstein DS, Eisenhofer G, Garty M, Sax FL, Keiser HR, Kopin IJ. Pharmacologic and tracer methods to study sympathetic function in primary hypertension. *Clin Exp Hyper* 1989;A11 (suppl. 1):173–189.
5. Ziegler MG, Lake CR, Kopin IJ. The sympathetic-nervous-system defect in primary orthostatic hypotension. *N Engl J Med* 1977;296:293–297.
6. Goldstein DS, Polinksy RJ, Garty M, et al. Patterns of plasma levels of catechols in neurogenic orthostatic hypotension. *Ann Neurol* 1989;26:558–563.
7. Imperato-McGinley J, Gautier T, Ehlers K, Zullo MA, Goldstein DS, Vaughan ED Jr. Reversibility of catecholamine-induced dilated cardiomyopathy in a child with pheochromocytoma. *N Engl J Med* 1987;316:793–797.
8. Greenhoot JH, Reichenbach DD. Cardiac injury and subarachnoid hemorrhage. *J Neurosurg* 1969;30:521–531.
9. Goldstein DS, Keiser HR. Neural circulatory control in the hyperdynamic circulatory state syndrome. *Am Heart J* 1985;109:387–390.
10. Goldstein DS, Spanarkel M, Pitterman A, Toltzis R, Gratz E, Epstein S, Keiser HR. Circulatory control mechanisms in vasodepressor syncope. *Am Heart J* 1982;104:1071–1075.
11. Glass DS, Krakoff LR, Contrada R, et al. Effect of harassment

and competition upon cardiovascular and plasma catecholamine responses in type A and type B individuals. *Psychophysiology* 1980;17:453–463.
12. Deka-Starosta A, Garty M, Zukowska-Grojec Z, Keiser HR, Kopin IJ, Goldstein DS. Renal sympathetic nerve activity and norepinephrine release in rats. *Am J Physiol* 1989;257:R229–R236.
13. Goldstein DS, McCarty R, Polinsky RJ, Kopin IJ. Relationship between plasma norepinephrine and sympathetic neural activity. *Hypertension* 1983;5:552–559.
14. Goldstein DS, Brush JE Jr, Eisenhofer G, Stull R, Esler M. In vivo measurement of neuronal uptake of norepinephrine in the human heart. *Circulation* 1988;78:41–48.
15. Esler M, Jennings G, Korner P, et al. Assessment of human sympathetic nervous system activity from measurements of norepinephrine turnover. *Hypertension* 1988;11:3–20.
16. Dae MW, O'Connell JW, Botvinick EH, et al. Scintigraphic assessment of regional cardiac innervation. *Circulation* 1989;79:634–644.
17. Sisson JC, Shapiro B, Meyers L, et al. Metaiodobenzylguanidine to map scintigraphically the adrenergic nervous system in man. *J Nucl Med* 1987;28:1625–1636.
18. Wieland DM, Brown LE, Rogers WL, et al. Myocardial imaging with a radioiodinated norepinephrine storage analog. *J Nucl Med* 1983;24:1127–1134.
19. Chiueh CC, Zukowska-Grojec Z, Kirk KL, Kopin IJ. 6-fluorocatecholamines as false adrenergic neurotransmitters. *J Pharmacol Exp Ther* 1983;225:529–533.
20. Eisenhofer G, Hovevey-Sion D, Kopin IJ, et al. Neuronal uptake and metabolism of 2- and 6-fluorodopamine: false neurotransmitters for positron emission tomographic imaging of sympathetically innervated tissues. *J Pharmacol Exp Ther* 1989;248:419–427.
21. Goldstein DS, Chang PC, Eisenhofer G, et al. Positron emission tomographic imaging of cardiac sympathetic innervation and function. *Circulation* 1990;81:1606–1621.
22. Weil-Malherbe H, Axelrod J, Tomchick R. Blood-brain barrier for adrenaline. *Science* 1959;129:1226–1227.
23. Garnett ES, Firnau G, Nahmias C. Dopamine visualized in the basal ganglia of living man. *Nature* 1983;305:137–138.
24. Harvey J, Firnau G, Garnett ES. Estimation of the radiation dose in man due to 6-[^{18}F] Fluoro-L-dopa. *J Nucl Med* 1985;26:931–935.
25. Kirk KL, Cantacuzene D, Nimitikitpaisan Y, et al. Synthesis and biological properties of 2-, 5- and 6-fluoro-norepinephrine. *J Med Chem* 1979;22:1493–1497.
26. Kirk KL. Photochemistry of diazonium salts. 4. Synthesis of ring-fluorinated tyramines and dopamines. *J Org Chem* 1976;41:2373–2376.
27. Eisenhofer G, Goldstein DS, Stull R, et al. Simultaneous liquid chromatographic determination of 3,4-dihydroxyphenylglycol, catecholamines, and 3,4-dihydroxyphenylalanine in plasma, and their responses to inhibition of monoamine oxidase. *Clin Chem* 1986;32:2030–2033.
28. Eisenhofer G, Kirk KL, Kopin IJ, Goldstein DS. Simultaneous determination of endogenous catechols and exogenous 2- and 6-fluorinated catechols in tissue and plasma using liquid chromatography with electrochemical detection. *J Chromatog* 1988;431:156–162.
29. Van Schaik FW, Van Heeswijk GM, Huisman GH. Uptake and metabolism of catecholamines in the awake dog. *Arch Int Physiol Biochim* 1985;93:339–349.
30. Goodall McC, Alton H. Metabolism of 3-hydroxytyramine (dopamine) in human subjects. *Biochem Pharmacol* 1968; 17:905–914.
31. Axelrod J. The fate of adrenaline and noradrenaline. In: Vane JR, Wolstenholme GEW, O'Connor M, eds. *Adrenergic mechanisms.* Boston, MA: Little, Brown and Company; 1960:28–39.
32. Kirshner N. The metabolism of [^{14}C](±)-adrenaline in the cat. In: Vane JR, Wolstenholme GEW, O'Connor M, eds. *Adrenergic mechanisms.* Boston, MA: Little, Brown and Company: 1960:45–55.
33. Hovevey-Sion D, Eisenhofer G, Kopin IJ, et al. Metabolic fate of injected [^{3}H]-dopamine and [^{3}H]-2-fluorodopamine in rats. *Neuropharmacology* 1990;29:881–887.
34. Goldstein DS, Horwitz D, Keiser HR, Polinsky RJ, Kopin IJ. Plasma ^{3}H-l-norepinephrine, ^{14}C-d-norepinephrine, and ^{3}H-d,l-isoproterenol kinetics in essential hypertension. *J Clin Invest* 1983;72:1748–1758.
35. Iversen LL. Catecholamine uptake processes. *Br Med Bull* 1973;29:130–135.
36. Shargel L, Yu ABC. *Applied biopharmaceutics and pharmacokinetics.* Norwalk, CN: Appleton-Century-Crofts; 1985.
37. Gryglewski R, Vane JR. The inactivation of noreadrenaline and isoprenaline in dogs. *Br J Pharmacol* 1970;39:573–584.
38. Zimlichman R, Goldstein DS, Eisenhofer G, Stull R, Keiser HR. Comparison of noradrenaline and isoprenaline removal in the canine hindlimb and kidney. *Clin Exp Pharmacol Physiol* 1986;13:777–781.
39. Hempel K, Lane HW, Kayser EF, Roger L, Hennemann H, Heidland A. Role of O-methylation in the renal excretion of catecholamines in dogs. *Naunyn-Schmiedeberg's Arch Pharmacol* 1973;277:373–386.
40. Micalizzi ER, Pals DT. Evaluation of plasma norepinephrine as an index of sympathetic neuron function in the conscious, unrestrained rat. *Life Sci* 1978;24:2071–2076.
41. Goldstein DS, Nurnberger J Jr, Gershon ES, Simmons S, Polinsky R, Keiser HR. Effects of injected sympathomimetic amines on plasma catecholamines and circulatory variables in man. *Life Sci* 1983;32:1057–1063.
42. Iversen LL, Glowinski J, Axelrod J. The physiologic disposition and metabolism of norepinephrine in immunosympathectomized animals. *J Pharmacol Exp Ther* 1966;151:273–284.
43. Guyton AC. *Textbook of medical physiology* Philadelphia: WB Saunders; 1986.
44. McPhee MS, Greenberger NJ. Diseases of the gallbladder and bile ducts. In: Braunwald E, Isselbacher KJ, Petersdorf RG, Wilson JD, Martin JB, Fauci AS, eds. *Harrison's principles of internal medicine.* New York, NY: McGraw-Hill Book Co.; 1987:1358–1368.
45. Andersen AC, Good LS, eds. *The beagle as an experimental dog.* Ames, Iowa: The Iowa State University Press; 1970.
46. Shepherd JT, Vanhoutte PM. *The human cardiovascular system. Facts and concepts.* New York: Raven Press; 1979.
47. Coffey JL, Watson EE. S values for selected radionuclides and organs with the heart wall and heart contents as source organs. Oak Ridge Associated Universities, Oak Ridge, TN.